American Mineralogist, Volume 74, pages 360–366, 1989

Iron distribution and structural order in synthetic calcic amphiboles studied by Mössbauer spectroscopy and HRTEM

HENRIK SKOGBY*
Department of Mineralogy and Petrology, Institute of Geology, Uppsala University, Box 555, S-751 22 Uppsala, Sweden
EMBAIE FERROW
Department of Mineralogy and Petrology, Institute of Geology, Lund University, Sölvegatan 13, S-223 62 Lund, Sweden

ABSTRACT

Temperature-dependent cation distribution among the four nonequivalent M(1) to M(4) positions in synthetic calcic amphibole has been studied by means of Mössbauer spectroscopy. Both stoichiometric and Ca-deficient compositions, with low Fe/Mg ratios, have been synthesized and annealed using hydrothermal techniques. Structural homogeneity of the run products was confirmed by use of high-resolution transmission electron microscopy (HRTEM). Results from Mössbauer spectroscopy reveal that Fe^{2+} is always present on the M(4) site, including the results for the stoichiometric composition that was expected to show the M(4) site entirely occupied by Ca. With decreasing temperature, Fe^{2+} increases on the M(4) site, decreases on the M(2) site, and remains constant on the M(1) + M(3) sites. The exchange of Fe^{2+} between the M(2) and M(4) sites is probably coupled with an exchange of Mg in the opposite direction by the disordering reaction $Fe^{2+}_{M(4)} + Mg_{M(2)} = Mg_{M(4)} + Fe^{2+}_{M(2)}$, in analogy with earlier studies of natural tremolite-actinolite. The HRTEM studies reveal a high degree of structural order in the synthetic calcic amphiboles, in contrast to earlier work on synthetic Fe-Mg-Mn amphiboles where high concentrations of chain-width disorder and stacking faults have been found. These results imply that the composition influences the amount of structural imperfections found in synthetic amphiboles.

INTRODUCTION

Cation distribution among the four nonequivalent M(1) to M(4) sites in natural calcic amphiboles has been studied by X-ray single-crystal refinements (Papike et al., 1969; Mitchell et al., 1971; Ungaretti et al., 1983) and spectroscopic methods (Burns, 1970; Burns and Greaves, 1971). Mössbauer spectroscopy of actinolite has demonstrated the presence of Fe^{2+} on the M(4) site (Goldman, 1979). Usually this site is assumed to be completely occupied by Ca in ideal tremolite-actinolite ($Ca_2(Mg,Fe)_5Si_8O_{22}(OH)_2$). Fe^{2+} on the M(4) site of calcic amphiboles has also been confirmed by X-ray structure refinements (e.g., Ungaretti et al., 1983). The accommodation of Fe^{2+} and Mg on the large M(4) site in calcic amphibole reflects solubility of a grunerite-cummingtonite component. In fact, Wones and Dodge (1977), on surveying over 1200 amphibole analyses, observed only 9 analyses that were close to the Ca end-member composition. These authors also reported the formation of diopside and quartz in synthesis experiments starting with the ideal tremolite composition, indicating that stoichiometric tremolite may not be a stable phase above 700 °C. Incomplete yields of synthetic calcic amphiboles with formation of pyroxene have also been reported by Oba (1980), Oba and Nicholls (1986), and Raudsepp et al. (1987). In a recent paper, Jenkins (1987) concluded that pressure, temperature, growth rate, and bulk composition are not limiting factors in attempts to synthesize ideal tremolite and that synthetic tremolite always has a cummingtonite component of about 10%.

As pointed out by Maresch and Czank (1983b), a number of studies of synthetic amphiboles have led to conflicting results regarding stabilities and phase relations. Such results could be due to small-scale structural defects that cannot be detected by conventional techniques. HRTEM studies on synthetic Fe-Mg-Mn amphiboles by these authors revealed two types of structural defects at the unit-cell scale, chain-multiplicity faults (CMFs) and chain-arrangement faults (CAFs). CMFs occur when the number of subchains that are linked to form a multiple chain is different from the two of normal double-chain amphibole structures. This type of defect has also been called chain-width disorder and has been extensively described in natural amphiboles (Veblen and Buseck, 1979, 1980). CAFs are faults in the stacking sequence of the chains in the a^* direction. This type of defect is usually (100) twin planes and can cause synthetic monoclinic amphibole to appear orthorhombic in optical and X-ray studies.

Maresch and Czank (1983b) suggested that many synthetic amphiboles may have higher concentrations of CMFs and CAFs than their natural counterparts and

* Present address: California Institute of Technology, Division of Geological and Planetary Sciences, Pasadena, California 91125, U.S.A.

0003–004X/89/0304–0360$02.00

thereby have different stabilities and phase relations. CMFs commonly decrease the M(4)/[M(1) + M(2) + M(3)] ratio to less than the ideal ⅖ by formation of "wide-chain pyribole." Because M(4) is the only site that can accept Ca, the resulting "pyribole" is unable to accommodate as much Ca as the ideal double-chain amphibole. In synthesis experiments, the compositional change causes a residual composition equivalent to diopside to be left over from a starting mixture of tremolite composition. High concentrations of CMFs in synthetic calcic amphiboles could in this way explain the problems in obtaining the Ca end-member.

Exchange of Fe^{2+} and Mg among the nonequivalent octahedral positions in the amphibole structure has been studied in natural Fe-Mg and calcic amphiboles. Using hydrothermal techniques and Mössbauer spectroscopy, Skogby and Annersten (1985) and Skogby (1987) showed that the Fe-Mg exchange in calcic amphiboles occurs between the M(2) and M(4) sites only, following the disordering reaction

$$Fe^{2+}_{M(4)} + Mg_{M(2)} = Mg_{M(4)} + Fe^{2+}_{M(2)}. \quad (1)$$

In the present paper we describe further study of the Fe^{2+} distribution and exchange in synthetic calcic amphibole produced under controlled temperatures and with special emphasis on the Ca content. This study is restricted to calcic amphiboles with low Fe content, which give well-resolved low-temperature Mössbauer spectra from which the distribution of Fe among the M(1) + M(3), M(2), and M(4) sites can be determined. Structural homogeneity of the synthetic and annealed phases is confirmed using HRTEM.

Experimental procedure

Synthesis

Three different calcic amphibole compositions were prepared for the synthesis experiments, one with M(4) = 2.00 Ca,

$$Ca_{2.00}Fe_{0.35}Mg_{4.65}Si_{8.00}O_{22}(OH)_2,$$

and two Ca-deficient compositions,

$$Ca_{1.92}Fe_{0.35}Mg_{4.73}Si_{8.00}O_{22}(OH)_2$$

and

$$Ca_{1.75}Fe_{0.65}Mg_{4.60}Si_{8.00}O_{22}(OH)_2.$$

The starting material consisted of oxide mixtures of reagent-grade Fe_2O_3, CaO, MgO, and SiO_2. After mixing, the charges were heated in a H_2 atmosphere until the red color of Fe_2O_3 disappeared, reducing the Fe^{3+} to Fe^{2+}. The oxide mixtures were then seeded with 6 wt% natural actinolite (sample 679, Skogby and Annersten, 1985) and thoroughly mixed by grinding in acetone. Approximately 180-mg portions of these mixtures were then sealed in Au capsules, together with 15 wt% doubly distilled water. The capsules were checked for leakage by weighing before and after each run. Buffering techniques were not used, but the Ni-containing alloy of the pressure vessels is assumed to give an oxygen fugacity comparable to the NNO buffer. In addition, the degree of Fe oxidation in the run products was determined by the subsequent Mössbauer analysis.

Table 1. Experimental conditions and results from synthesis runs

Run	Starting composition in M sites	T (°C)	Duration (days)	Run products
		Synthesis experiments		
8	$Ca_{2.00}Fe_{0.35}Mg_{4.65}$	500	148(2)	Tr(85) + Tlc(5) + Di(10)
7		600	92(1)	Tr(96) + Cum(2) + Di(2)
4	$Ca_{1.92}Fe_{0.35}Mg_{4.73}$	500	189(4)	Tr(96) + Tlc(3) ± Cum
2		600	105(2)	Tr(97) + Tlc(3)
6		700	87(1)	Tr(97) + Fo(2) ± Cum
10	$Ca_{1.75}Fe_{0.65}Mg_{4.60}$	500	184(2)	Tr(95) + Tlc(3) ± Cum ± Di
9		600	112(1)	Tr(99) ± Cum
		Annealing experiments		
13	$Ca_{1.92}Fe_{0.35}Mg_{4.73}$	800	3	Tr(100)
15		750	4	Tr(100)
17		700	6	Tr(100)
19		650	8	Tr(100)
14	$Ca_{1.75}Fe_{0.65}Mg_{4.60}$	800	3	Tr(98) + Cum(2)
16		750	4	Tr(98) + Cum(2)
18		700	6	Tr(97) + Cum(3)
20		650	8	Tr(96) + Cum(4)

Note: The charges were seeded by 6 wt% natural tremolite. Compositions are given for M sites only; for total composition $Si_{8.00}O_{22}(OH)_2$ should be added. The digit in parentheses in the "duration" column denotes the number of times the charge was restarted. Run products in estimated percentage of the detected phases, as obtained from X-ray diffraction. ± denotes amounts smaller than 2%. Abbreviations: Tr = tremolite-actinolite; Tlc = talc; Di = diopside; Cum = cummingtonite (or anthophyllite); Fo = forsterite.

The experiments were performed in cold-sealed pressure vessels at 2-kbar pressure and temperatures of 500 to 800 °C. All samples were ground and rerun up to four times to improve the amphibole yield. The first run periods were started by a fast increase in temperature to 850 °C (in about 1 h). The charges were kept at 1 kbar and 850 °C for 4 h before the actual run temperature and pressure were established. This procedure was used to avoid formation of metastable talc. The temperature was continuously recorded, and the errors in temperature and pressure are estimated to be ±0.1 kbar and ±5 °C respectively. All experiments were quenched in a stream of compressed air, resulting in a temperature drop of about 200 °C/min. Experimental conditions and run products are shown in Table 1.

Phase identification and characterization

The run products were analyzed by X-ray powder diffraction after each run using Ni-filtered $Cu_{K\alpha}$ radiation. After the first period of hydrothermal heating, multiphase products were common. Even though amphibole was the dominating phase, talc and diopside were also present. Minor amounts of forsterite and Fe-Mg amphibole also occurred. Because there was only one weak reflection due to Fe-Mg amphibole (d = 3.05 Å), it was not possible to determine whether this phase represents monoclinic cum-

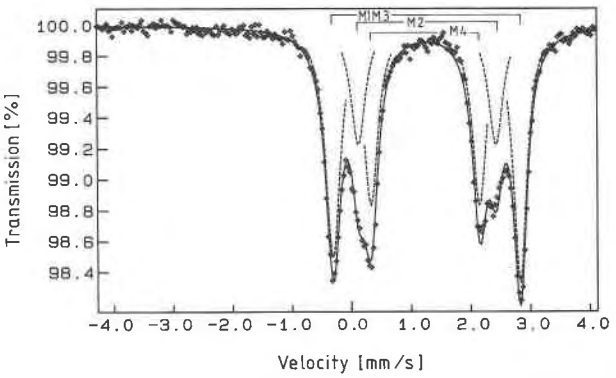

Fig. 1. Mössbauer spectrum of synthetic calcic amphibole (run 20) obtained at 77 K.

mingtonite (d_{310}) or orthorhombic anthophyllite (d_{610}). Repeated grinding and hydrothermal heating improved the amphibole yield.

To estimate the detection limits for other phases present in the synthetic products, mixtures of synthetic amphibole with natural talc, diopside, and anthophyllite were prepared and studied by X-ray diffraction. Minimum detection limits were 1–2 wt% for talc and about 2–4 wt% for the other phases. X-ray data for these mixtures were also used to estimate the modal abundances of the phases obtained.

Cell parameters of the final calcic amphiboles were calculated using a least-squares fitting program and the 10 peaks suggested by Cameron (1975) for characterization of amphiboles. The diffraction patterns were calibrated against an external Si standard.

Most of the final synthetic products were studied by HRTEM, using a Philips EM 400T instrument operated at 100 kV and equipped with a field-emission gun source. Samples were prepared by suspending the synthetic amphibole on C-coated Cu grids (Veblen, 1985). Image interpretation followed the procedure described by Veblen and Buseck (1979, 1980).

Mössbauer spectroscopy was used to determine the distribution of Fe among the different octahedral positions in the amphibole structure. All measurements were made with the sample kept at liquid-N_2 temperature, which increases spectral resolution for amphiboles. The measurements and the fitting procedure of the spectra were similar to those described by Skogby and Annersten (1985), with assignment of the absorption doublets as suggested by Goldman (1979) and indicated in Figure 1.

Fe-site occupancies were calculated from the area ratios of the absorption doublets and the Fe content of the charges. It is important to note that in the runs that did not result in a pure calcic amphibole product, other Fe-containing phases present will add to the absorption pattern of the calcic amphibole. Talc has a very low solubility of Fe and will not contribute appreciably to the spectra. Diopside has a higher solubility of Fe, but has Mössbauer parameters different from those of the calcic amphibole (Bancroft et al., 1971). Diopside patterns were not detected in any spectra. Coexisting synthetic cummingtonite and actinolite contain roughly the same amount of Fe (Cameron, 1975), but the Fe in cummingtonite is strongly fractionated to the M(4) site (Hafner and Ghose, 1971). Therefore, cummingtonite co-existing with calcic amphibole will considerably increase the absorption doublet of the M(4) site, and run products containing cummingtonite will not represent the true Fe distribution for the calcic amphibole.

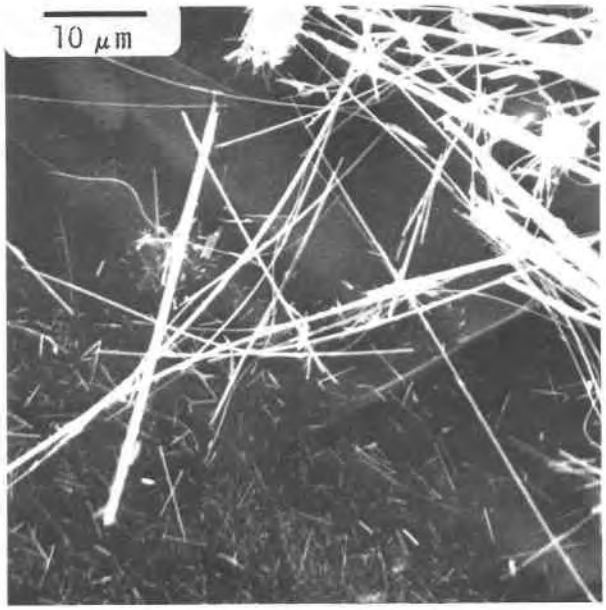

Fig. 2. Scanning-electron-microscopy image of calcic amphibole synthesized at 500 °C (run 10).

Results and discussion

Hydrothermal run products

Acceptable yields of synthetic tremolite-actinolite could be obtained only after hydrothermal runs 2–6 months long (Table 1). Highest yields were obtained for Ca-deficient compositions. For the composition with Ca = 2.00 synthesized at 500 °C, the amphibole yield was only 85% after 148 d of heating, and appreciable amounts of diopside and talc remained. The synthetic amphibole crystals are commonly 0.3 × 5 μm in size, but longer fibers occur in run products at 500 °C (Fig. 2).

For annealing experiments with the Ca = 1.92 composition, the products from runs 4 and 6 were mixed, annealed at 800 °C for 3 d, and then subsequently at lower temperatures. The durations of the experiments were long enough to ensure intracrystalline equilibrium according to a kinetic study on natural tremolite (Skogby, 1987). This procedure resulted in very pure amphibole products (Table 1).

The same procedure was repeated for runs 9 and 10 of the most Ca-deficient composition ($Ca_{1.75}$), but these annealing runs also contained a Fe-Mg amphibole. This result indicates that the bulk composition is in the misci-

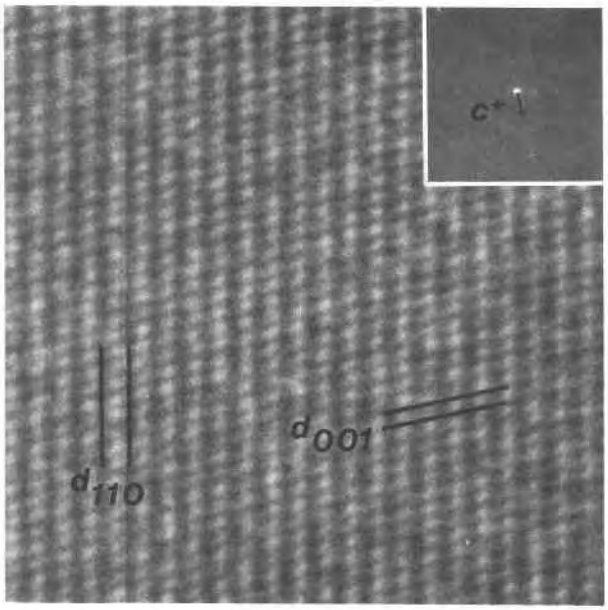

Fig. 3. HRTEM image of synthetic amphibole (run 4) viewed along the [110] direction. The bright spots correspond to "tunnels" of low electron density, i.e., the vacant A-positions on line in the viewing direction (cf. Fig. 4). The planes d_{001} = 5.11 Å and d_{110} = 8.41 Å are indicated.

bility gap in the amphibole quadrilateral (cf. Cameron, 1975). With decreasing annealing temperature, the amount of exsolved Fe-Mg amphibole increases, reflecting the increasing miscibility gap at lower temperatures.

Refined amphibole cell parameters were obtained for the run products with the highest amphibole yield for each composition (cf. Table 2). The Fe/Mg ratios and Ca contents were estimated using the method of Cameron (1975). In this method the b-axis dimension is used to determine the Fe/Mg ratio, and the β angle and the d_{100} value are used to determine the average radius of the ions occupying the M(4) site. The small range of compositions for the present synthetic calcic amphiboles is almost within the precision of the method. Even so, the b-axis dimension increases with increasing Fe/Mg ratio of the starting mixture, and the β angle decreases with increasing initial Ca content (Table 2). However, the d_{100} value method to estimate the Ca end-member component (Cameron, 1975) gives values 15–20% lower than the starting composition and Mössbauer spectroscopy. This discrepancy could be due to the large difference in Fe/Mg ratio for the present samples compared to those the method was calibrated against and suggests that the method is not generally applicable for measuring compositions of synthetic calcic amphiboles.

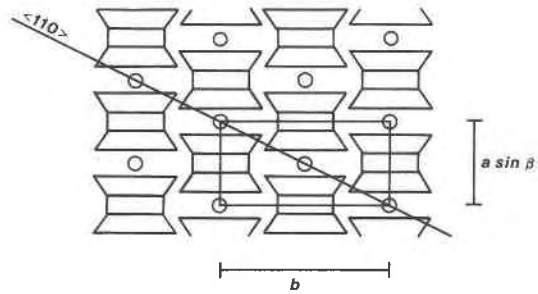

Fig. 4. Schematic projection of I-beam modules in the amphibole structure and the viewing direction [110] in Fig. 2. Circles represent the vacant A-positions.

Electron microscopy

HRTEM study of the samples described here reveal a much higher degree of structural order than for the previously studied Fe-Mg-Mn amphiboles (Maresch and Czank, 1983a, 1983b). CMFs occur only sporadically in the approximately 50 studied structure images (Figs. 3–7). Nevertheless, there is weak streaking in the $0k0$ direction of the electron-diffraction patterns for a few amphibole crystals. Because of orientation problems, the [010] direction required for the study of CAFs occurred only rarely, and in these cases, no stacking defects were observed. As discussed by Maresch and Czank (1983b), it is difficult to quantify the average state of structural disorder for a synthetic product. The disordered volume in the present samples is, however, estimated to be significantly less than a few percent. Thus, the concentration of the four different octahedral sites should be close to ideality. Compositional changes due to chain-mutliplicity faults should, therefore, not occur for the studied samples.

Mössbauer spectroscopy

All the amphiboles synthesized have Fe^{2+} distributed over all four octahedral sites (Fig. 1, Table 3). A few runs contain minor amounts of Fe^{3+}, which is assumed to occupy the M(2) position (Skogby and Annersten, 1985). The $X^{Fe^{2+}}_{M(4)}$ site occupancy is not well correlated with Ca deficiency of the starting mixture (note that runs 9 and

TABLE 2. Cell parameters for synthetic calcic amphiboles

Run	Starting composition in M sites	a (Å)	b (Å)	c (Å)	β (°)	V (Å^3)	Fe_{calc} (p.f.u.)
7	$Ca_{2.00}Fe_{0.35}Mg_{4.65}$	9.832(4)	18.078(10)	5.279(3)	104.62(4)	908.0(14)	0.42(17)
17	$Ca_{1.92}Fe_{0.35}Mg_{4.73}$	9.820(3)	18.079(6)	5.282(2)	104.59(3)	907.5(9)	0.44(10)
18	$Ca_{1.75}Fe_{0.65}Mg_{4.60}$	9.821(3)	18.089(6)	5.284(2)	104.51(3)	908.7(9)	0.61(10)

Note: Cell parameters were refined using a least-squares fitting program and the 10 peaks suggested by Cameron (1975). Values within brackets are calculated standard deviation of the last digit. Fe_{calc} is Fe atoms per formula unit in actinolite calculated from the b-axis dimension. The diffraction patterns were calibrated against an external Si standard.

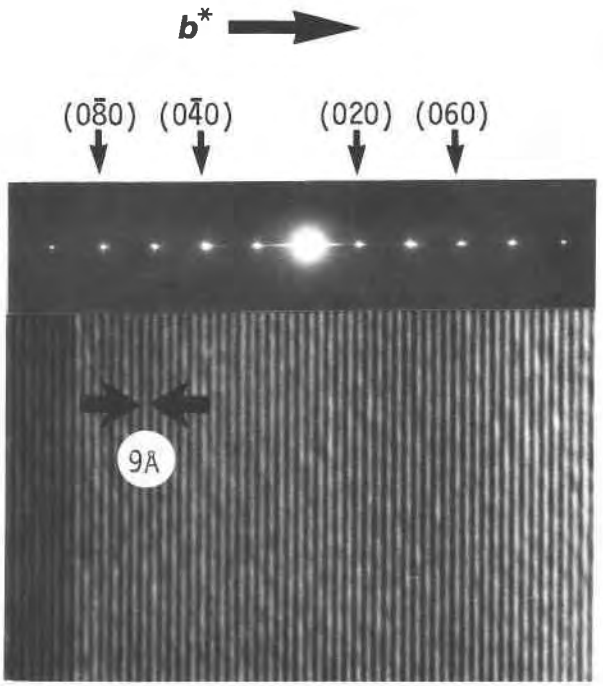

Fig. 5. HRTEM image of (0k0) fringes and diffraction pattern of synthetic amphibole (run 10), viewed in a direction perpendicular to the b axis. The bright fringes correspond to the centers of the amphibole double chains. The diffraction pattern shows weak streaking due to chain-multiplicity faults.

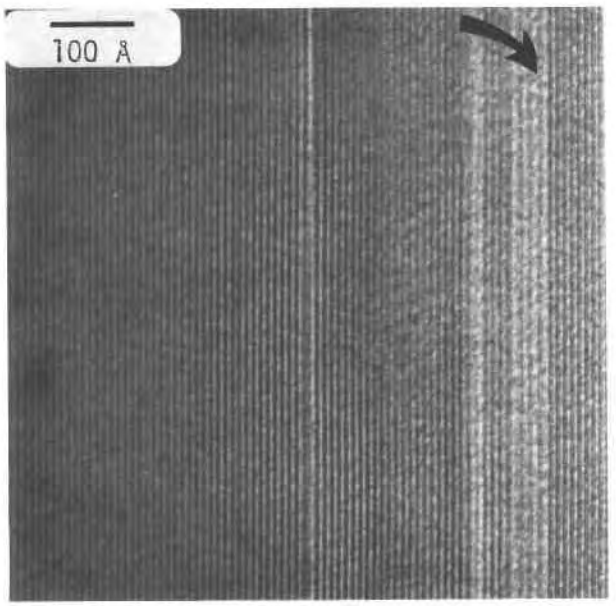

Fig. 6. HRTEM image showing chain-multiplicity faults (arrow) corresponding to triple chains (run 8).

10 have higher total Fe). According to Jenkins (1987), synthetic Fe-free tremolite has a fixed composition close to $X^{Ca}_{M(4)} = 0.90$, independent of starting composition. Since the present data indicate $X^{Fe^{2+}}_{M(4)}$ site occupancies of 0.04–0.06 for the two most Ca-rich compositions, and this site also will contain some Mg, an $X^{Ca}_{M(4)}$ value close to 0.90 is also reasonable for Fe-bearing tremolite-actinolite.

The distribution of Fe in the samples synthesized at 500 °C is not completely consistent with earlier results from experiments on natural actinolite-tremolite (Skogby and Annersten, 1985). The most important difference is that for the natural samples, Fe^{2+} is strongly ordered on the M(4) site at lower temperatures, whereas synthetic samples grown at 500 °C are not ordered to the same extent. This result might suggest that the amphiboles synthesized at 500 °C grew under nonequilibrium conditions regarding the Fe^{2+} intracrystalline distribution.

TABLE 3. Fe site occupancies for synthetic calcic amphibole obtained from Mössbauer spectroscopy

Run	Starting composition in M sites	T (°C)	$X^{Fe^{2+}}_{M(2)}$	$X^{Fe^{2+}}_{M(4)}$	$X^{Fe^{2+}}_{M(1)M(3)}$	$X^{Fe^{3+}}_{M(2)}$	ln K_D
			Synthesis experiments				
8	$Ca_{2.00}Fe_{0.35}Mg_{4.65}$	500	0.0544	0.0390	0.0527	0.0022	
7		600	0.0374	0.0617	0.0494	0.0017	
4	$Ca_{1.92}Fe_{0.35}Mg_{4.73}$	500	0.0403	0.0437	0.0602	—	
2		600	0.0425	0.0321	0.0637	0.0041	
6		700	0.0277	0.0609	0.0546	0.0038	
10	$Ca_{1.75}Fe_{0.65}Mg_{4.60}$	500	0.0679	0.0945	0.1061	0.0032	
9		600	0.0526	0.1241	0.0988	—	
			Annealing experiments				
13	$Ca_{1.92}Fe_{0.35}Mg_{4.73}$	800	0.0470	0.0547	0.0485	—	−3.20
15		750	0.0437	0.0553	0.0506	—	−3.30
17		700	0.0388	0.0582	0.0520	—	−3.54
19		650	0.0350	0.0633	0.0511	—	−3.86
14	$Ca_{1.75}Fe_{0.65}Mg_{4.60}$	800	0.0682	0.1183	0.0923	—	
16		750	0.0614	0.1225	0.0940	—	
18		700	0.0552	0.1274	0.0949	—	
20		650	0.0481	0.1387	0.0918	—	

Note: The spectra were obtained at liquid-N_2 temperature. The distribution coefficient is defined as

$$K_D = [X^{Fe^{2+}}_{M(2)}(1 - X^{Ca}_{M(4)} - X^{Fe^{2+}}_{M(4)})]/[(1 - X^{Fe^{2+}}_{M(2)})X^{Fe^{2+}}_{M(4)}],$$

where a fixed $X^{Ca}_{M(4)}$ value of 0.90 is used.

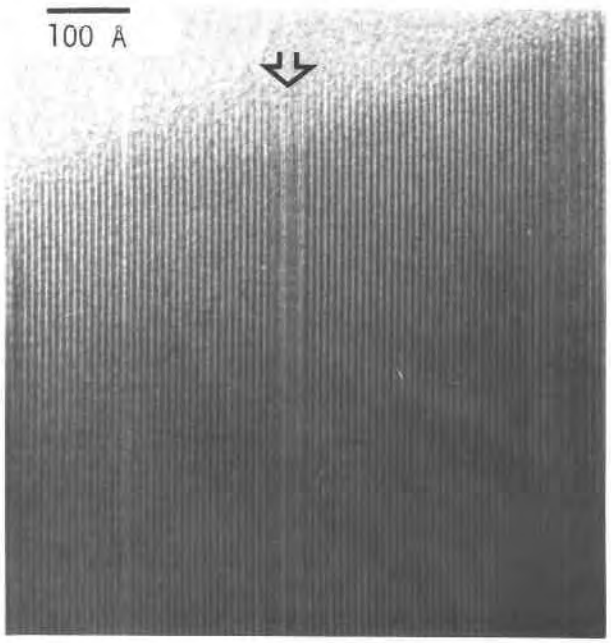

Fig. 7. HRTEM image of run 4. Arrow indicates a talc-like slab in the amphibole structure with multiplicity $m = 11$. The repeating distance of the subchains, 4.5 Å, is barely visible.

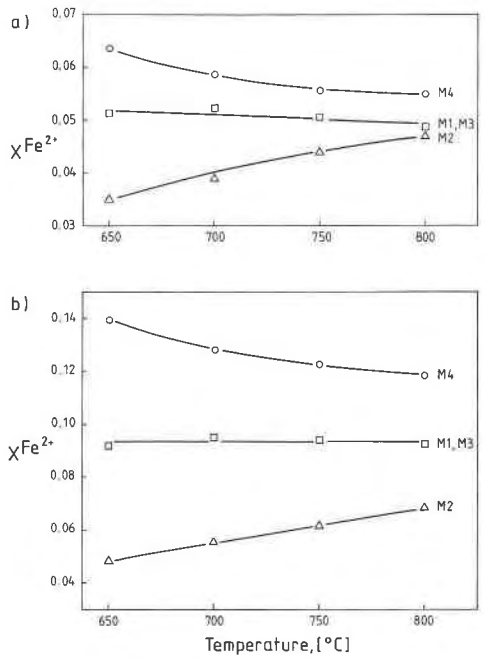

Fig. 8. Site occupancy of Fe^{2+} in annealed synthetic calcic amphibole. (**a**) Composition $Ca_{1.92}Fe_{0.35}Mg_{4.65}Si_{8.00}O_{22}(OH)_2$, runs 13, 15, 17, and 19. Only calcic amphibole was detected by X-ray diffraction. (**b**) Composition $Ca_{1.75}Fe_{0.65}Mg_{4.60}Si_{8.00}O_{22}(OH)_2$, runs 14, 16, 18, and 20. Calcic amphibole and small amounts of Fe-Mg amphibole were detected by X-ray diffraction. The amount of Fe-Mg amphibole increases from about 2 to 4% with decreasing temperature in the run series.

Intracrystalline exchange

For the two annealed compositions, it can be seen that Fe^{2+} increases on M(4) and decreases on M(2) with decreasing temperature, whereas Fe^{2+} remains approximately constant on M(1) + M(3) (Fig. 8). This behavior is the same as in experiments with natural actinolites-tremolites (Skogby and Annersten, 1985), which showed that Fe-Mg exchange occurs only between M(2) and M(4). The most Ca-deficient composition ($Ca_{1.75}$, runs 14, 16, 18, 20) also yields a slightly increasing amount of Fe-Mg amphibole with decreasing temperatures (from 2 to 4 wt%). The increase in M(4) intensity for these runs is accentuated by exsolved Fe-Mg amphibole, and these results do not represent a precise intracrystalline distribution for the calcic amphibole.

As for the natural tremolite, the exchange of Fe^{2+} between the M(2) and M(4) sites is probably coupled with exchange of Mg in the opposite direction, following disordering Reaction 1. Because of the compositional uncertainty, it is not possible to calculate the amount of Mg on M(4) only on the basis of starting composition and the Fe-site occupancies. However, if the fixed $X^{Ca}_{M(4)}$ site occupancy of 0.90 suggested by Jenkins (1987) is assumed, an estimate of $X^{Mg}_{M(4)}$ *can be calculated as* $X^{Mg}_{M(4)} = 1 - X^{Fe^{2+}}_{M(4)} - X^{Ca}_{M(4)}$. With this assumption, distribution coefficients defined as

$$K_D = \frac{X^{Fe^{2+}}_{M(2)}(1 - X^{Fe^{2+}}_{M(4)} - X^{Ca}_{M(4)})}{(1 - X^{Fe^{2+}}_{M(2)})X^{Fe^{2+}}_{M(4)}} \qquad (2)$$

were calculated for the annealed samples of composition $Ca_{1.92}$. For these annealing experiments (runs 13, 15, 17, 19), ln K_D values and corresponding data for natural actinolite (Skogby, 1987) are plotted versus $1/T$ in Figure

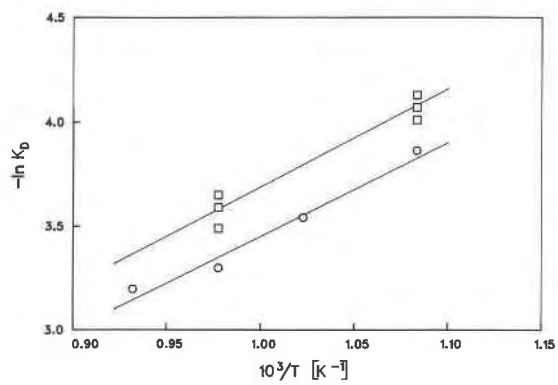

Fig. 9. Equilibrium Fe^{2+} distribution among M(4) and M(2) sites in synthetic (circles) and natural (squares) calcic amphibole. The distribution coefficient is defined as: $K_D = [X^{Fe^{2+}}_{M(2)}(1 - X^{Fe^{2+}}_{M(4)} - X^{Ca}_{M(4)})]/[(1 - X^{Fe^{2+}}_{M(2)})X^{Fe^{2+}}_{M(4)})]$. The data for the natural amphibole represents actinolite from Zillertal (Skogby and Annersten, 1985). The lines represent least-squares fits to the experimental data, yielding correlation coefficients of $r^2 = 0.99$ for synthetic samples and $r^2 = 0.97$ for natural samples.

9. If the activity coefficients for Fe and Mg on M(2) and M(4) are assumed to be equal to unity, these K_D values will equal equilibrium constants for order-disorder Reaction 1, and the slope of the lines will correspond to the enthalpy difference (ΔH^0) between the ordered and antiordered states (Seifert, 1978).

These ΔH^0 values are 8.9 kcal/mol for the synthetic samples and 9.2 ± 1.5 kcal/mol for the natural tremolite. The essentially identical values indicate a similar intracrystalline ordering behavior of Fe and Mg, although we must emphasize the large uncertainty for the synthetic samples arising mainly from the estimation of $X^{Mg}_{M(4)}$ discussed above.

Conclusions

The results from the HRTEM studies of hydrothermally synthesized calcic amphiboles show that it is possible to synthesize such amphiboles with low concentrations of chain-multiplicity faults (CMFs). The failures in attempts to synthesize the Ca end-member are not due to high concentrations of CMFs, and the doubt about the stability of calcic amphibole with M(4) = 2.00 Ca (e.g., Jenkins, 1987) is supported by the present study. It seems that the incorporation of Ca on the M(4) site of the amphibole structure increases the small-scale structural order (fewer CMFs), compared to Fe-Mg-Mn amphiboles. However, the comparatively large Ca ion does not completely fill all M(4) positions, possibly because of strain effects in the structure, which can be reduced by substitution of the smaller Fe and Mg ions.

The decreasing solubility of Fe-Mg amphibole in calcic amphiboles with decreasing temperature is confirmed, in agreement with the results of Cameron (1975) for compositions richer in Fe. The starting composition with Ca = 1.75 atoms per formula unit is within the miscibility gap but very close to the calcic amphibole field at 800 °C.

The intracrystalline Fe^{2+}-Mg distributions in synthetic and natural calcic amphiboles show the same temperature dependence. Exchange of Fe^{2+} and Mg occurs between M(2) and M(4), with Fe^{2+} increasing on M(4) as temperature decreases and Fe^{2+} on M(1) + M(3) remaining constant.

Acknowledgments

We are grateful to Drs. H. Annersten, M. Czank, and M. Roots for critical review of the manuscript. The HRTEM studies were conducted at the National Center for HREM in Lund and at the Biomedical Center in Uppsala. We are grateful to Dr. R. Wallenberg for assistance at the microscope.

References cited

Bancroft, G.M., Williams, P.G.L., and Burns, R.G. (1971) Mössbauer spectra of minerals along the diopside-hedenbergite tie line. American Mineralogist, 56, 1617–1625.

Burns, R.G. (1970) Mineralogical applications of crystal field theory, 244 p. University Press, Cambridge.

Burns, R.G., and Greaves, C.J. (1971) Correlations of infrared and Mössbauer site population measurements in actinolite. American Mineralogist, 56, 2010–2033.

Cameron, K.L. (1975) An experimental study of actinolite-cummingtonite phase relations with notes on the synthesis of Fe-rich anthophyllite. American Mineralogist, 60, 375–390.

Goldman, D.S. (1979) A reevaluation of the Mössbauer spectroscopy of calcic amphiboles. American Mineralogist, 64, 109–118.

Hafner, S.S., and Ghose, S. (1971) Iron and magnesium distribution in cummingtonites $(Fe,Mg)_7Si_8O_{22}(OH)_2$. Zeitschrift für Kristallographie, 133, 301–323.

Jenkins, D.M. (1987) Synthesis and characterization of tremolite in the system H_2O-CaO-MgO-SiO_2. American Mineralogist, 72, 707–715.

Maresch, W.V., and Czank, M. (1983a) Phase characterization of synthetic amphiboles on the join $Mn^{2+}_xMg_{7-x}(Si_8O_{22})(OH)_2$. American Mineralogist, 68, 744–753.

——— (1983b) Problems of compositional and structural uncertainty in synthetic hydroxyl-amphiboles. Periodico di Mineralogia, 52, 463–542.

Mitchell, J.T., Bloss, D., and Gibbs, G.V. (1971) Examination of the actinolite structure and four $C/2m$ amphiboles in terms of double bonding. Zeitschrift für Kristallographie, 133, 273–300.

Oba, T. (1980) Phase relations in the tremolite-pargasite join. Contributions to Mineralogy and Petrology, 71, 247–256.

Oba, T., and Nicholls, I.A. (1986) Experimental study of cummingtonite and Ca-Na amphibole relations in the system Cum-Act-Pl-Qz-H_2O. American Mineralogist, 71, 1354–1365.

Papike, J.J., Ross, M., and Clarke, J.R. (1969) Crystal-chemical characterization of clinoamphiboles based on five new structure refinements. In J.J. Papike, Ed., Pyroxenes and amphiboles: Crystal chemistry and phase petrology, p. 117–136. Mineralogical Society of America Special Paper 2.

Raudsepp, M., Turnock, A.C., Hawthorne, F.C., Sheriff, B.L., and Hartmann, J.S. (1987) Characterization of synthetic pargasitic amphiboles $(NaCa_2Mg_4M^{3+}Si_6Al_2O_{22}(OH)_2$; M^{3+} = Al, Cr, Ga, Sc, In) by infrared spectroscopy, Rietveld structure refinement, and ^{27}Al, ^{29}Si, and ^{19}F MAS NMR spectroscopy. American Mineralogist, 72, 580–593.

Seifert, F.A. (1978) Equilibrium Mg-Fe^{2+} cation distribution in anthophyllite. American Journal of Science, 278, 1323–1333.

Skogby, H. (1987) Kinetics of intracrystalline order-disorder reactions in tremolite. Physics and Chemistry of Minerals, 14, 521–526.

Skogby, H., and Annersten, H. (1985) Temperature dependent Mg-Fe-cation distribution in actinolite-tremolite. Neues Jahrbuch für Mineralogie Monatshefte, 193–203.

Ungaretti, L., Lombardo, B., Domeneghetti, C., and Rossi, G. (1983) Crystal-chemical evolution of amphiboles from eclogitised rocks of the Sesia-Lanzo Zone, Italian Western Alps. Bulletin de Minéralogie, 106, 645–672.

Veblen, D.R. (1985) High-resolution transmission electron microscopy. In J.C. White, Ed., Mineralogical Association of Canada Short Course in Application of Electron Microscopy in the Earth Sciences, 63–88.

Veblen, D.R., and Buseck, P.R. (1979) Chain-width order and disorder in biopyriboles. American Mineralogist, 64, 687–700.

——— (1980) Microstructures and reaction mechanisms in biopyriboles. American Mineralogist, 65, 599–623.

Wones, D.R., and Dodge, F.C.W. (1977) The stability of phlogopite in the presence of quartz and diopside. In D.G. Frazer, Ed., Thermodynamics in geology, p. 229–247. Reidel, Dordrecht, Netherlands.

Manuscript received April 18, 1988
Manuscript accepted November 23, 1988